

DOI: <http://doi.org/10.52716/jprs.v11i4.563>

Synthesis and Characterization of High Surface Area Nano Titanium Dioxide

Dalya Jasim Ahmed^{1,*}, Basim Ibrahim Al-abdaly², Sattar Jalil Hussein³

^{1,3}Iraqi Ministry of Oil, Petroleum Research & Development Center

²Department of Chemistry, College of Science, University of Baghdad, Baghdad, Iraq.

^{1,*} Corresponding Author E-mail: dalyairaq207@yahoo.com

basim.ibrahim@sc.uobaghdad.edu.iq, sattarjalil.fr@gmail.com

Received 15/3/2021, Accepted 21/6/2021, Published 20/12/2021



This work is licensed under a [Creative Commons Attribution 4.0 International License](https://creativecommons.org/licenses/by/4.0/).

Abstract

TiO₂ and TiO₂-Al₂O₃ nanoparticles were synthesized via sol-gel method using hydrolysis of Titanium tetraisopropoxide (TTIP) with ethanol and water mixture as titania source. TiO₂-Al₂O₃ Nano-composite was successfully synthesized using the sol-gel technique. Tetraisopropoxide and aluminium isopropoxide were used to prepare TiO₂-Al₂O₃. All prepared samples calcination were conducted at different temperature (400 to 700) °C. The synthesized TiO₂ and TiO₂-Al₂O₃ nanocomposites were then characterized by XRD, AFM, BET surface area, SEM, XRF. XRD, the analysis showed that the presence of alumina (Al₂O₃) in the TiO₂ has an effect on crystal size, particles size, surface area, and crystal phases; The XRD result revealed that the prepared TiO₂ nanoparticles were anatase phase at 400oC, and 500oC, and transformed to rutile from 600oC to 700oC, but after addition of alumina TiO₂ was of anatase phase, without any rutile at all calcination temperatures, also, the addition of alumina leads to a significant decrease in the crystal size, particles size, especially at high temperatures while the surface area of pure titanium was increased, and this corresponds to the results of the AFM and SEM. The best-obtained surface area was 355.18 m²/ gm. with 34.98 nm of average particle size at 500oC in comparison with pure nano titanium dioxide.

Keywords: TiO₂, Nanoparticles, Sol-gel, Anatase, Al₂O₃

تحضير وتشخيص جسيمات نانوية لثاني أكسيد التيتانيوم بمساحة سطحية عالية

الخلاصة:

تم تحضير الجسيمات النانوية TiO_2 و $TiO_2-Al_2O_3$ باستخدام طريقة sol-gel و التحلل المائي لرباعي أكسيد التيتانيوم (TTIP) مع خليط الإيثانول والماء كمصدر للتيتانيا. تم تصنيع المركبات النانوية $TiO_2-Al_2O_3$ بنجاح بطريقة sol-gel. و استخدام التيتانيوم (IV) رباعي الأيزوبروبوكسيد وأيزوبروبوكسيد الألومنيوم لتحضير $TiO_2-Al_2O_3$. تم إجراء الكلسنة لجميع العينات المحضرة عند درجات حرارة مختلفة (400 إلى 700) م وأجريت عمليات التشخيص لـ TiO_2 و $TiO_2-Al_2O_3$ المركب النانوي بواسطة XRD، AFM، المساحة السطحية BET، SEM، XRF، XRD، كشفت تحاليل تشتت الأشعة السينية ان الجسيمات النانوية لأكسيد التيتانيوم المحضر هي من طور الاناتاييس بدرجة 400 و 500 م° وتتحول الى طور الروتيل بدرجة 600 الى 700 م أظهرت التحاليل أن وجود الألومينا (Al_2O_3) في TiO_2 له تأثير على حجم البلورة وحجم الجسيمات ومساحة السطح وحجم المسام للمساحيق المكونة والمراحل البلورية؛ وكان TiO_2 المحضر من طور anatase، بدون أي روتيل في جميع درجات حرارة التكليس. أدت إضافة الألومينا إلى زيادة معنوية في مساحة سطح التيتانيوم النقي وكانت أفضل مساحة تم الحصول عليها 355.18 م² / غم. بمتوسط حجم جسيمي يبلغ 34.98 نانومتر عند 500 درجة مئوية مقارنة بثاني أكسيد التيتانيوم النقي.

الكلمات المفتاحية: أكسيد التيتانيوم، الدقائق النانوية، سول-جل، اناتاييس، أكسيد الألمنيوم.

1. Introduction

Metal oxide-based nanoparticles (MONPs) can adopt different structural geometries; therefore, it can exhibit versatile and potential applications in different areas including electronics, optical and life science in general such as; insulator and semiconductor character. Also, nanoparticles metals have unique physicochemical characteristics, when are comparing with bulk materials counterparts because of their "restricted" surface of high density and size [1].

Therefore, surface effects and interface effects become more important [2]. Technologically, oxides are used in piezoelectric devices, the fabrication of microelectronic circuits, fuel cells, sensors, and coatings for the passivation of surfaces against corrosion. And some of the metals oxides such as Fe, Co, Ni, Cu and Zn have many remarkable applications, including solar energy transformations, electronics, magnetic storage media, catalysis and semi-conductor [1].

In the promising field of nanotechnology, the main objective is to make nanostructures or nanoarrays with unique properties respecting those of single or bulk particle species [3]. Different metal oxide nanoparticles were used in the oil and gas industry in various fields such as filler or additive in drilling [4], enhanced oil recovery [5], and catalyst [6]. Among various kinds of metal oxide nanoparticles, the most commonly used are including Fe_2O_3 ,

SiO₂, Al₂O₃, MgO, ZrO₂, CeO₂, TiO₂, and ZnO [7]. These metal oxides are generally used as active metals (Mo and W) support in hydrodesulfurization, like TiO₂, ZrO₂ showed prominent activity, but some disadvantages are prevented their commercial exploitation like limited thermal stability, inappropriate mechanical properties and reduced surface area and low thermal stability. Many methods are used to overcome these disadvantages such as; mixed oxides to get the benefit of preferred features for both systems like mixed with γ -Al₂O₃, also some systems research to get understand the function of support in the reactions of hydrotreating such as mixed with SiO₂, MgO, ZrO₂, and B₂O₃ [8].

Titanium dioxide (TiO₂) has many properties such as chemical stability, low cost, easy handling, non-toxicity, and environment-friendly, this made it of great importance in the field of technology applications. Therefore, a lot is being driven to perform researches varied from the applications of energy to environmental ones that are dealing with catalytic features in these wide fields. TiO₂ is a semiconductor with a wide bandgap; it is exhibiting resistance to erosion in its two types of chemical and photochemical. These features make TiO₂ a substance widely used in chemical sensors, solar cells, hydrogen gas production, also as pigments, self-cleaning surfaces, and application of environmental purification [9]. Sulfur compounds are one of the most common impurities in crude oil which is widely used as transportation fuels such as gasoline, diesel and jet fuels [10].

Residual sulfur species in fuels will lead to the emission of sulfur oxide gases naturally, these gases react with water in the atmosphere to form sulfates and acid rain which can damage buildings, destroy automotive paint finishes, acidifies soil and ultimately lead to the destruction of forest and various other ecosystems [11]. Automobiles are also adversely affected by the presence of sulfur species in the fuels as the sulfur species have a profound effect on the efficacy of catalytic converters [12]. There are many processes applied to reduce sulfur content in refined petroleum liquid hydrocarbons [13]. The hydrodesulfurization method (HDS) is one of the most important and efficient methods of removing sulfur compounds from a petroleum stream [14], [15]. The γ -Al₂O₃ supported with Mo Oxide catalysts and promoted with Co or Ni is still used extensively in the process of sulfur compounds removal in the refining industry, γ -Al₂O₃ is very important among other phases because of its structure that possesses a high surface which gains the focus for many chemical and petrochemical separation processes and catalysis [16].

In recent years, many stringent environmental regulations have been issued, and this has led to an increased need for hydrodesulfurization (HDS) catalyst that is more active, effective, and different from the standard sulfide catalyst. Titanium oxide (TiO_2) is good new support for hydrotreating (HDT) catalysts [17], it improves the performance of catalyst for many reactions, such as dehydrogenation [18], [19], hydrodesulfurization [20], water-gas shift, and thermal catalytic decomposition [21]. But TiO_2 has the disadvantages of presenting poor thermal stability, a low value of a surface area, and bad mechanical properties.

There are several methods followed by some authors to overcome these disadvantages such as the grafting of TiO_2 with $\gamma\text{-Al}_2\text{O}_3$, SiO_2 , etc. TiO_2 with other mixed oxides to be formed such as SiO_2 , Al_2O_3 , and ZrO_2 . $\text{TiO}_2\text{-Al}_2\text{O}_3$ are among these mixed oxides systems that have received maximum attention while many researchers also studied $\text{TiO}_2\text{-ZrO}_2$ and $\text{TiO}_2\text{-SiO}_2$ is relatively less studied [22]., and an important requirement for improving the TiO_2 catalytic activity is to increase its specific surface area, this property is increased considerably through the high surface-to-volume ratio of the nanoparticles. (Nano-object with all three external dimensions in the Nanoscale or nanoscale, the size range for approximately 1nm to 100 nm) as compared to that of microparticles [23].

Authors in [24] were proposed $\text{TiO}_2\text{-Al}_2\text{O}_3$ mixed oxides as catalyst support. $\text{TiO}_2\text{-Al}_2\text{O}_3$ mixed oxides were prepared by sol-gel route using titanium and aluminium isopropoxides, chelated with acetylacetone to promote a similar hydrolysis ratio for both the alkoxides. The surface area was superior to $200 \text{ m}^2/\text{gm}$. and mean pore size of about 1nm. These characteristics of porous texture are preserved after firing at 673 K. The diffraction patterns of sample fired above 973K showed only the presence of anatase crystalline phase. The crystalline structure of the support remained unaltered after molybdenum adsorption, but the surface area and the micropore volume were drastically reduced.

The mesoporous TiO_2 from high specific surface area nanosheets was prepared by Athapon Author in [25], using a simple hydrothermal method at $120 \text{ }^\circ\text{C}$ of 12 h using an autoclave unit (Thai made). The shape, size by TEM, crystalline structure by XRD, BET-specific surface area and photocatalytic activity of the prepared samples were investigated. The specific surface area, average pore diameter and pore volume were $360.28 \text{ m}^2/\text{gm}$., 3-5 nm and $0.275 \text{ cm}^3/\text{gm}$. respectively. This work showed that the calcined nanosheets higher

photocatalytic activity than those of the as-synthesized sample and the commercial nano TiO₂ powders (P-25, JRC-01, JRC-03). Also, this synthesis method provided a simple route to fabricate nanostructures TiO₂ with high photocatalytic activity. Mehdi Karimi *et al.* (2013) [26] are synthesized High purity titanium dioxide (TiO₂) nanoparticles via the sol-gel method with surface area relatively 75.64m²/g, using titanium tetra-isopropoxide (TTIP), and synthesized material was used as a photocatalyst for the removal of mercaptans from gasoil. The XRD analysis showed that the product was TiO₂ nanoparticles in anatase form. The crystalline phase product was composed of fine particles with dimensions between 17 and 20 nm. The result showed that up to 78% of the mercaptans in gas-oil was removed using the synthesized TiO₂ photocatalyst.

The aim of this study is the preparation of TiO₂, and TiO₂-Al₂O₃ nanoparticles via a sol-gel technique, also this work focused on the effect of alumina addition on the crystal size, particles size, phase transformation, and surface area, as well as the effect of temperature on the properties of pure titanium and its comparison with TiO₂-Al₂O₃ mixed oxides. Where many uses and applications of nano titanium oxide are based on these properties.

2. Experimental

2.1 Synthesis of titanium dioxide nanostructures (TNPs) by Sol-Gel route

Synthesis of TiO₂ nanoparticles was accomplished by the Sol-gel route [27], making use of titanium tetra isopropoxide (TTIP), Ethyl alcohol (EtOH), HCL (36%), and distilled water as the starting materials. Preparation of solution (A) was made by using [TTIP: EtOH: H₂O: HCl] of volume ratio that was selected as (1:7:0.35:0.07). Titanium tetra isopropoxide Ti (OCH (CH₃)₂)₄ with (7 ml) was dissolved in (30 ml) of Ethyl alcohol at room temperature. In the meantime, a little volume of concentrated HCl (0.5 ml) was mixed with (20 ml) of anhydrous ethanol in addition to (2.5 ml) of water for preparing the solution (B). Solution (A) was thereafter dropwise added to the solution (B) under strong stirring for 30 min.

A homogeneous mixture solution was obtained after vigorous stirring for a period of 2 hours, where a sol was generated. After 24 hours, finally, the sol was converted into a gel to obtain nanoparticles, centrifugation process was used to separate the product at (5000 rpm for 15 min) which was finally dried at 100°C for 24 hours to ensure removing residual

organic material and water. The dried gel was annealed at 400°C for 4 hours (heating rate=3°C/min), to acquire the desired TiO₂ NPs.

2.2 Preparation of nano TiO₂-γAl₂O₃

The TiO₂-γAl₂O₃ was prepared through the sol-gel process previously reported by Wenjie Zhang et al. (2015) [28]., with modifications in starting materials, molar ratio, and calcination temperature. Titanium (IV) tetra isopropoxide Ti (OC₃H₇)₄ and aluminium isopropoxide (C₉H₂₁AlO₃) were used as a precursor for preparing alumina–titania nanopowder. preparing solution (A) was implemented by adding (3gm.) of aluminium isopropoxide to (50 ml) of isopropanol with stirring for 10 min., and then (12.5 ml) of titanium (IV) tetra isopropoxide was added to aluminium isopropoxide solution with stirring at (600 rpm) for 30 min. Meanwhile, (1 ml) of concentrated Hydrochloric acid (HCl) was mixed with (30 ml) of isopropanol and (10 ml) of deionized water to prepare the solution (B). Solution (A) was subsequently added gradually to the solution (B) under vigorous stirring within 30 min.

After stirring vigorously for 4 hours a homogeneous solution was obtained, and a sol was formed. After 48 hours of ageing time, the sol was finally transformed into a gel. Centrifugations at (5000 rpm for 15 min) were used to separate the product and obtain the nanoparticles. Then the product was subjected to drying at 100°C for 24 hours to ensure removing the water and residual organic material. The dried gel was annealed at 500°C for 3 hours (heating rate=3°C/min), to acquire the desired TiO₂-γAl₂O₃ nanoparticles.

3. Result and Discussion

3.1 Characterization of TiO₂ and TiO₂-Al₂O₃ Nanoparticles (TNPs)

3.1.1 X-Ray Diffraction (XRD)

The identity of the titanium dioxide (TiO₂), TiO₂-Al₂O₃, nanoparticles prepared at different temperature (400,500,600, and 700) °C that was determined by the X-ray diffraction technique.

The XRD pattern of the TiO₂ is observed to be in good agreement with the well-known reference pattern (JCPDS 21-1272) of TiO₂ [29]. Some researchers used the Scherrer equation to calculate particle size where the equation measures crystallite size [30].

$$D=K\lambda / (\beta\cos\theta) \dots\dots\dots (1)$$

In Figure (1) (a and b) (calcined at 400°C and 500°C) respectively, we can observe the formation of a single-phase and crystalline anatase with the sharp peak at $2\theta = 25.29^\circ$ and six small peaks at $2\theta = 38.095^\circ, 48.111^\circ, 53.990^\circ, 55.373^\circ, 62.770^\circ,$ and 70.542° .

It should be noted that only anatase TiO_2 [29], and there is no peak present assigned to the rutile phase ($2\theta = 27.360^\circ$) [31]. The peaks of the sample that was sintered at 500°C become much sharper revealing the formation of larger crystallites of anatase and the enhancement of crystallization.

It can be concluded from the calcination of 600°C Figure (1, c) a rutile phase was formed, and the peaks become sharper as the temperature of calcination is increased. This agrees with previous experiments [32]. In addition to the peaks of TiO_2 anatase, the peaks of TiO_2 rutile are found at $2\theta = 27.528^\circ, 36.142^\circ,$ and 41.339° and all peaks of TiO_2 rutile are in good agreement with the JCPDS card #75-1753 [33]. This suggests that at a temperature of about 600°C there is a phase transition from anatase to rutile which is in agreement with the last experiments. The TiO_2 anatase phase still exists in the sample at 600°C and 700°C. At 700°C [32] Figure 1(d) peaks of the rutile phase are become very strong and sharp at $2\theta = 27.210^\circ, 27.433^\circ, 35.789^\circ, 35.985^\circ,$ and 41.095° , with weak peaks for the anatase phase at $2\theta = 25.269^\circ,$ and 48.057° [34].

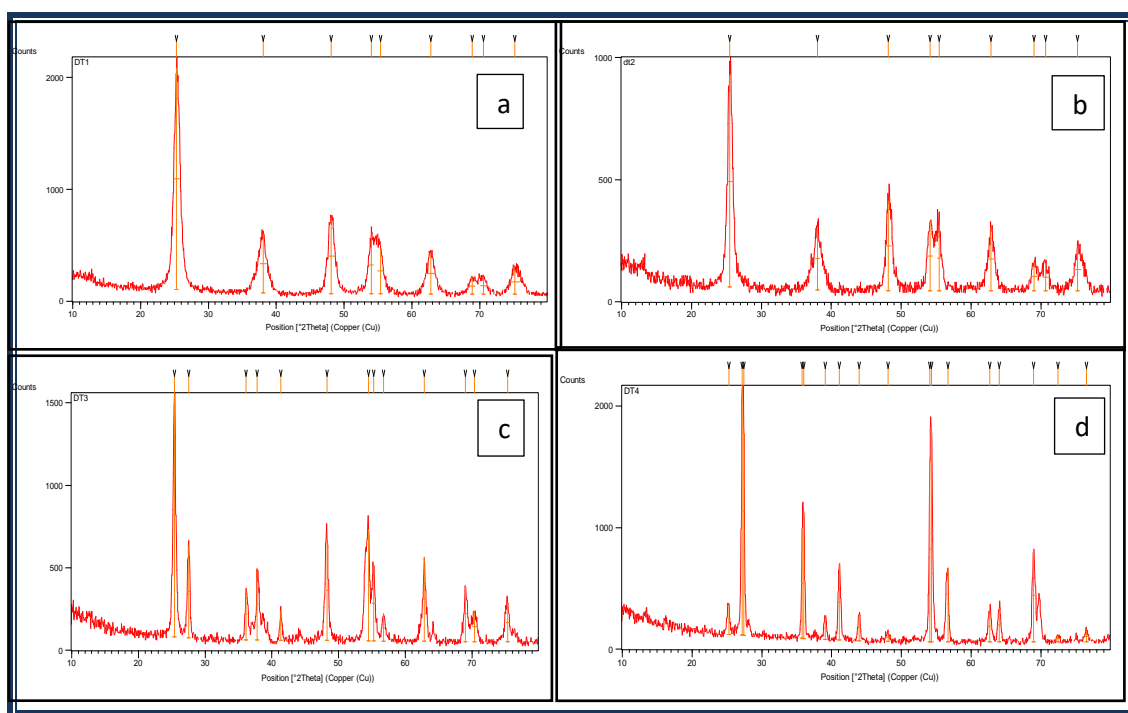


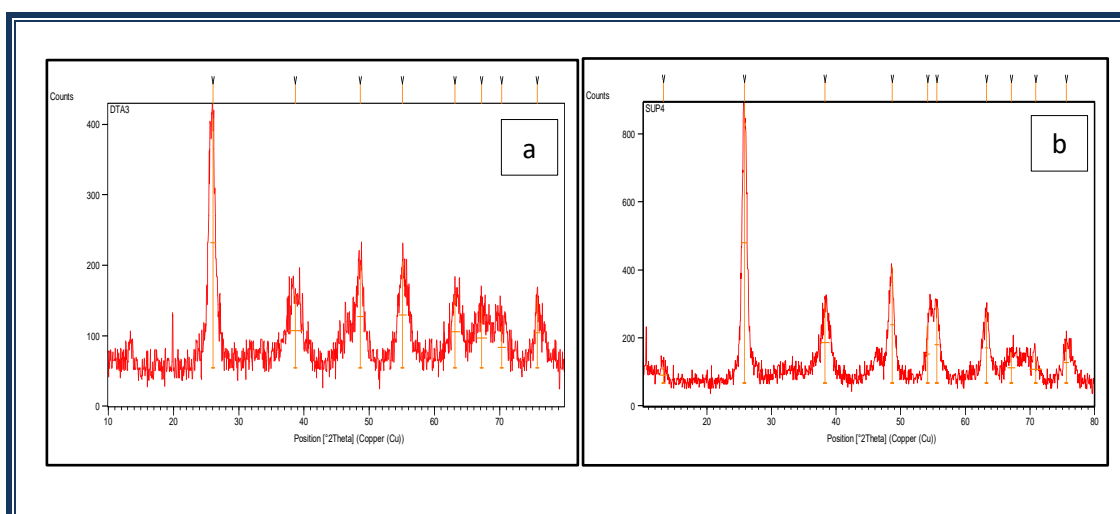
Fig. (1) XRD for TiO_2 , (a) at 400°C (b) at 500°C (c) at 600°C (d) at 700°C.

Crystallite sizes of anatase and rutile phases are listed in Table (1). It is seen that the crystallite size of pure TiO₂ of the anatase phase increases with increasing calcination temperatures from 400°C to 700°C [35]. That is because the particles' growth is induced by an increased temperature [32]. In single-phase anatase, the size of crystals increases from 9.24 nm to 12.03 nm when calcination temperatures are raised from 400°C to 500°C. The anatase phase is transformed to the rutile phase and rutile phase peaks appear at temperatures of between 600°C and 700°C and the crystallite size of more than 30 nm [34, 35].

Table (1) Crystallite sizes of anatase and rutile phases

Calcination temperature (°C)	Crystallite size for TiO ₂ (nm)		Particle size (nm)	Surface area (m ² /g)
	Anatase	Rutile		
400	9.20	-	32.50	104
500	12.03	-	40.38	96
600	32.40	24.58	44.70	76
700	37.22	42.60	58.40	47.75

The XRD patterns of TiO₂-Al₂O₃ (63% TiO₂, 32% Al₂O₃) mixed oxide prepared by sol-gel method calcined at (400, 500, 600, and 700) °C are shown in Figure 2(a- d).



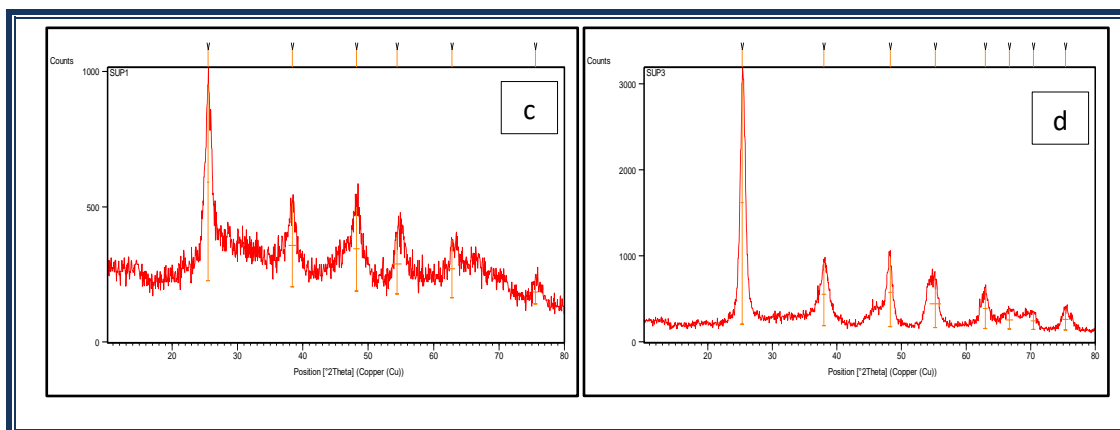


Fig. (2) XRD for $\text{TiO}_2\text{-Al}_2\text{O}_3$ (a) at 400°C (b) at 500°C (c) at 600°C (d) at 700°C .

Through the XRD of $\text{TiO}_2\text{-Al}_2\text{O}_3$ and its comparison with pure titanium, it was observed that the peaks in titanium were less wide, this refers that TiO_2 is a highly crystalline product, also has a low surface area [36]. With the decrease in the amount of titanium by adding of γ -alumina (Al_2O_3) for preparing $\text{TiO}_2\text{-Al}_2\text{O}_3$ mixed oxide, observed broader diffraction peaks, this means that the crystal size of titanium starts to decrease with the decrease in TiO_2 content in $\text{TiO}_2\text{-Al}_2\text{O}_3$ mixed oxide, meaning that alumina prevents the growth of crystal for titanium [36, 37], as it can be seen in table 2. The peaks' intensity increases as the temperature increase, while their width decreases [17]. Only the diffraction peaks of anatase appeared at all calcined temperatures from 400°C to 700°C , this means that no phase transformation had occurred [37]. Figure (3) showed the Effect of adding Al_2O_3 on crystal size for TiO_2 at different temperatures.

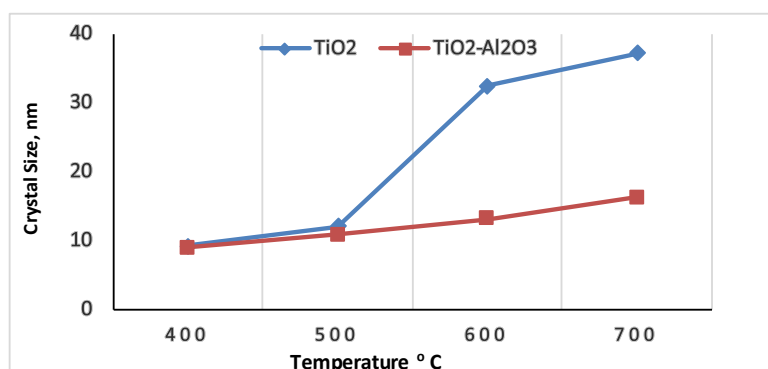


Fig. (3) Effect of adding Al_2O_3 on crystal size for TiO_2 at different temperatures.

Anatase TiO₂ typical peaks are present at $2\theta = 25^\circ, 38^\circ, 48^\circ, \text{ and } 54^\circ$, at temperature (400,500,600,700) °C, besides, some of the typical reflections of poorly crystalline γ -alumina can be seen at a calcined temperature 400°C and 500°C which can be observed at the $2\theta = 37^\circ, 46^\circ, 66^\circ, \text{ and } 67^\circ$ [38]. At the same time, the peak intensities of anatase TiO₂ are diminished obviously with the loading γ -alumina of (32 wt. %). This refers that there is a considerable modification effect on TiO₂ support with the presence of γ -alumina, which is obviously in line with the surface area results [38].

Table (2) Average crystal size, particles size, and surface area of the prepared particles

<i>Temperatures °c</i>	<i>Crystal size (nm)</i>	<i>Particles size (nm)</i>	<i>Surface area (m²/gm.)</i>
400	8.90	29.00	171.54
500	10.80	34.98	355.18
600	13.10	40.56	162.22
700	16.30	46.69	148.40

3.1.2 Scanning Electron Microscope (SEM)

The precursor TiO₂ nanoparticles morphologies and particle size distribution at different calcination temperatures (400, 500, 600, and 700) °C obtained by the sol-gel method is indicated in the SEM micrographs as shown in Figure (4). The obtained SEM images revealed that the particles of synthesized TiO₂ samples were in the range of nano size, at temperature 400°C particle-sized TiO₂ samples consist of (32.5) nm spherical particles as shown in figure 4a. When the temperature increases, the sizes become bigger and the agglomeration becomes significant.

It was observed that the large particle size is obtained at higher calcination temperatures, the particle size (58.4) nm is for the samples calcined at 700°C [32]. Figure (4d). The obtained results are in good agreement with XRD results showing that the particle size of the rutile phase is greater than that of the anatase phase due to the aggregation of nanoparticles with increasing calcination temperature.

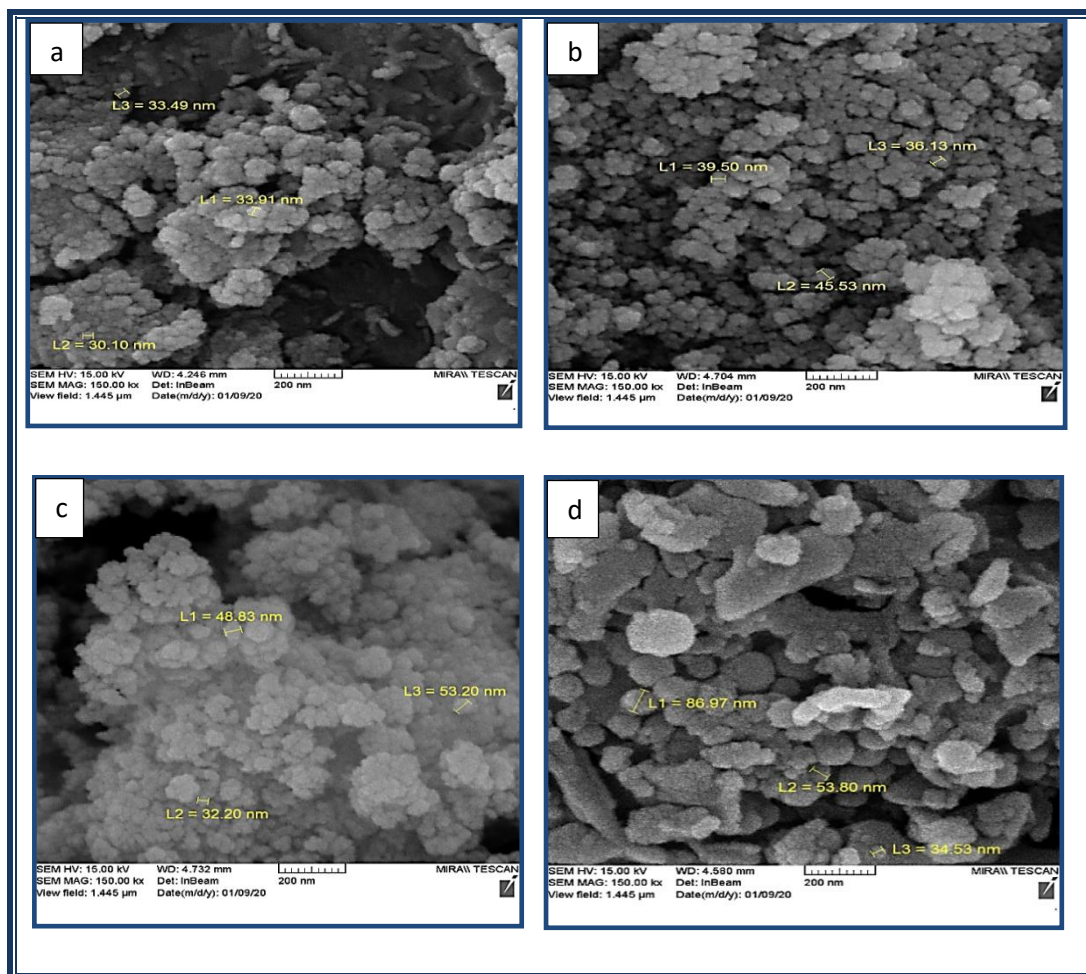


Fig. (4) SEM for TiO₂ (a) at 400° C (b) at 500° C (c) at 600° C (d) at 700° C.

The surface morphologies of TiO₂-Al₂O₃ composite materials for different calcination temperatures (400, 500, 600, and 700) °C obtained by the sol-gel method are shown in Figure (5). The obtained SEM images indicate that the particles of synthesized TiO₂-Al₂O₃ samples were in the nano-sized range. The Scherrer equation has been used to measure the crystallite size of the composite titania-alumina nanoparticles [39]. For all calcination temperatures (400,500,600,700) °C the crystal, and particle size for composite TiO₂-Al₂O₃ decreases when compared with pure TiO₂, at the same time they are increased with an increase in temperature [36], [39] as shown in Table (2), that may be due to the addition of alumina that can inhibit the aggregation of TiO₂ particles [37].

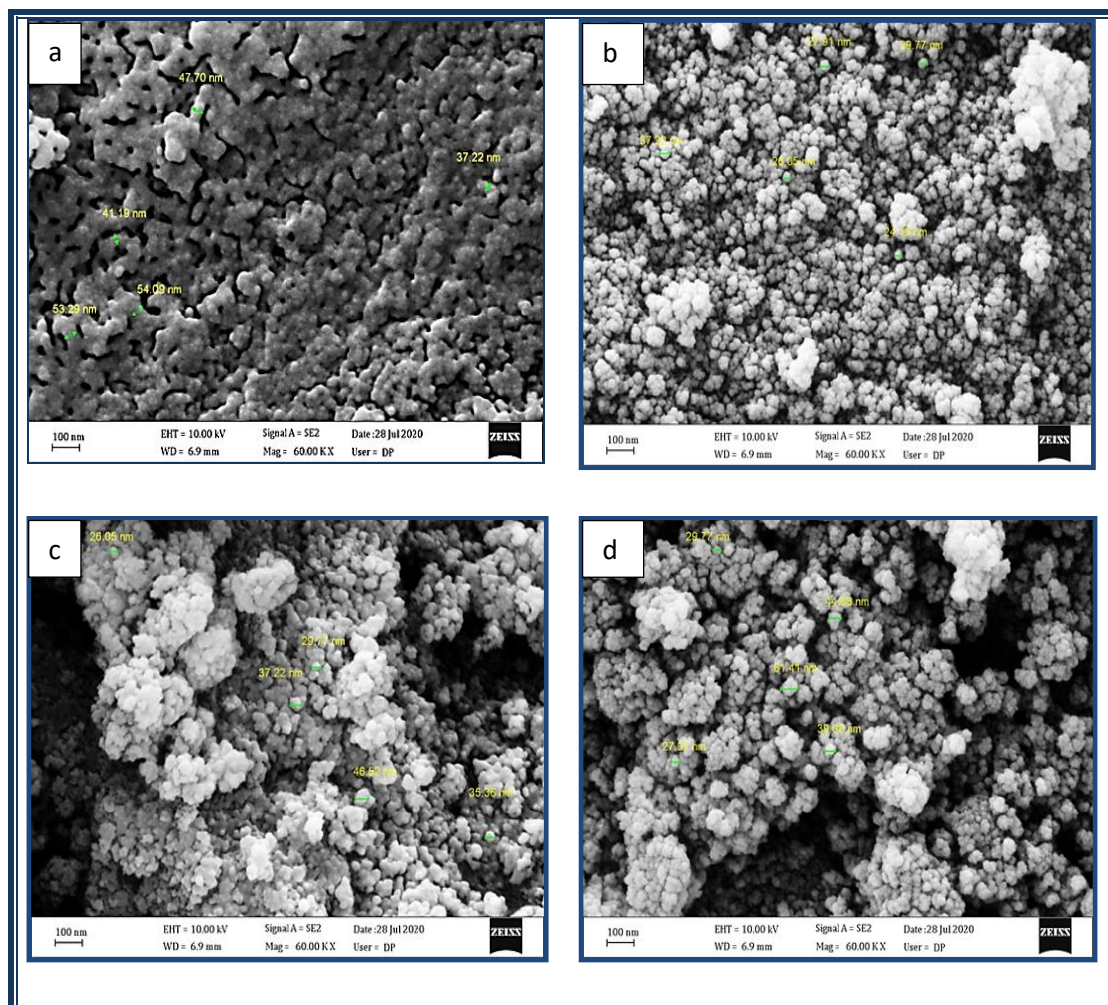


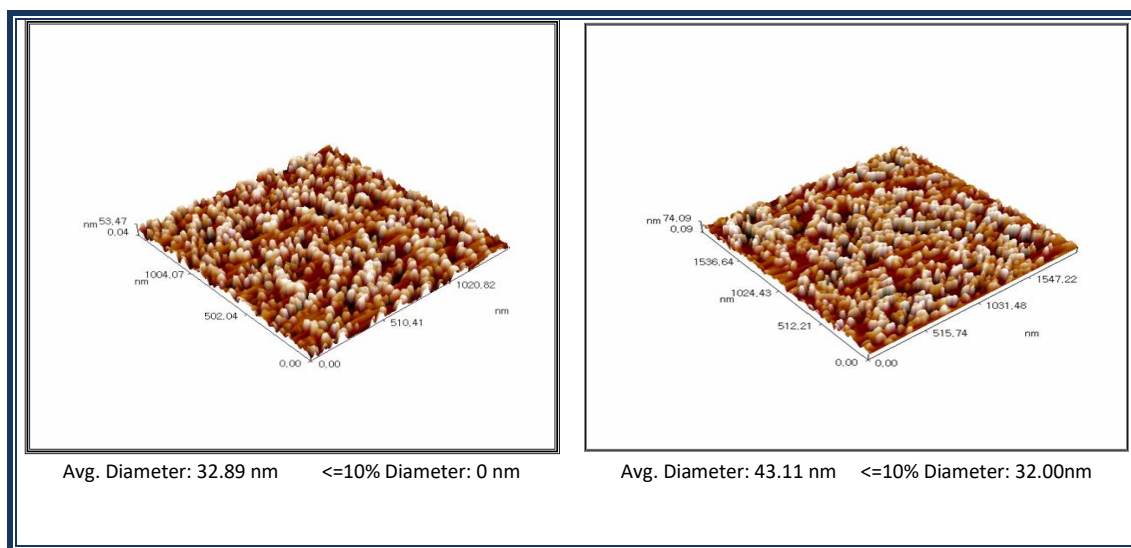
Fig. (5) SEM for $\text{TiO}_2\text{-Al}_2\text{O}_3$ mixed oxide (a) at 400°C (b) at 500°C (c) at 600°C (d) at 700°C .

Surface morphology is very important for the activity of the materials, and some properties can provide more active centers such as rough and structured surfaces with high surface area [40]. The chemical composition of the samples was analyzed by XRF the results indicated the chemical composition was 32% Al_2O_3 , 64% TiO_2 .

3.1.3 Atomic Force Microscopy (AFM)

The atomic force microscopy (AFM) technique was used to find the distribution of average particle size, and shape of the surface. The AFM images in three dimensions and distribution of average particle view of TiO_2 nanoparticles at different temperatures (400, 500, 600, and 700) $^\circ\text{C}$, are shown in Figure (6, a - d) respectively.

The average particle size of the prepared nano titania was in the nanoscale for all experiments. Increasing the calcination temperature from 400°C to 700°C leads to an increase in the particle size from 32.89 nm to 63.76nm. Increasing the calcination temperature from (400-700) °C leads to large changes in topography and roughness of the TiO₂ due to increasing the particle size of nano TiO₂ form, and to the phase shift of titanium anatase to rutile [32]. Table (1) shows the AFM (3D) images show that the temperature affects the size of TiO₂ grains significantly. At 400°C annealing temperature, Figure (6a), the surface morphology indicates a fine structure with a small grain size in the anatase phase. However, at 700°C (fig. 6d), larger TiO₂ crystal grains are observed [41]. The AFM results are in good agreement with the SEM, and XRD findings, which show the dependence of structural changes on thermal annealing [32],[41]. At 600°C and 700°C large crystal, grains are observed. The maximum average grain size obtained at 700°C was about 63.76 nm.



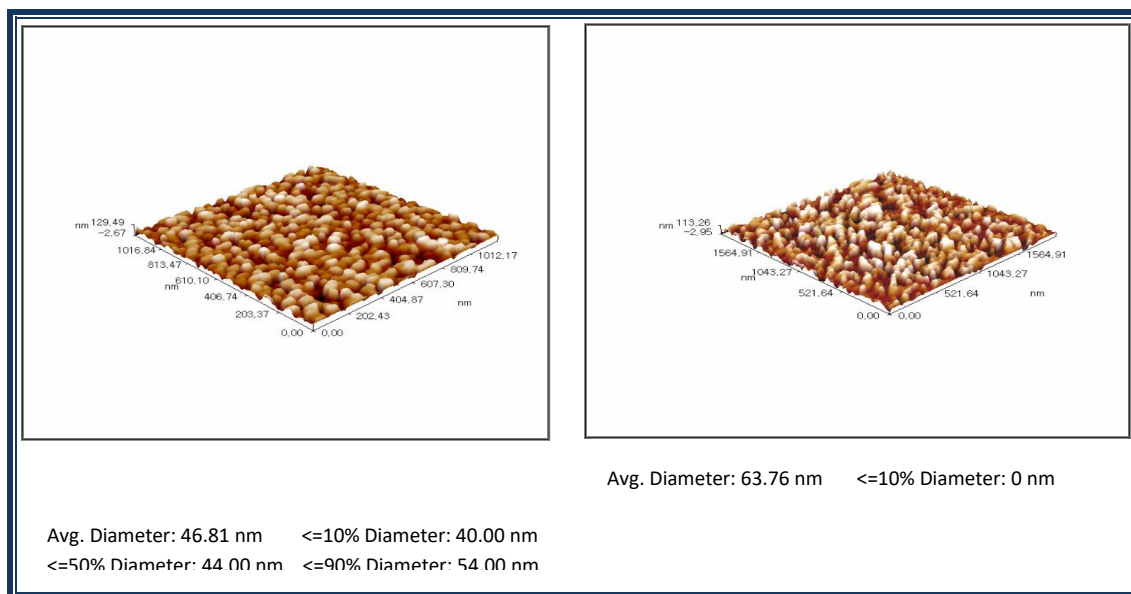


Fig. (6) (3D and particles distribution) AFM of TiO₂ nanoparticles

(a) at 400°C, (b) at 500°C, (c) at 600°C, (d) 700°C

Figure 7, (a to d) showed the AFM for TiO₂-Al₂O₃ composed at calcination temperatures (400,500,600,700) °C respectively. Generally, when comparison with TiO₂ observed that the presence of Al₂O₃ improves surface morphology of pure TiO₂ (surface roughness), the surface becomes flatter; it is observed that the result obtained through AFM is close to what was obtained in the SEM [42].

AFM analysis of the nano composed TiO₂-Al₂O₃ was performed to get a better understanding of the calcination temperature effect. All experiments showed an average particle size of the prepared nano titania in the nanoscale. It was observed that increasing calcination temperature from 400°C to 700°C leads to an increase in the particle size ranged from 41.52 nm to 47.78 nm. At higher annealing temperatures bigger clusters come to appear and granular structure has occurred with the effect of better crystallization [43]. The particles size at a temperature of 700°C is greater than the other (47.78) nm, which is maybe due to the amorphous phase of TiO₂, and Al₂O₃ [43]., it is observed that the result obtained through AFM is close to what was obtained in the XRD. In figures 7(a to d) respectively it can be seen that there is a change in morphology as the annealing temperature increases, although this change was gradually and slightly, the roughness indicates that the effect of better crystallization [43].

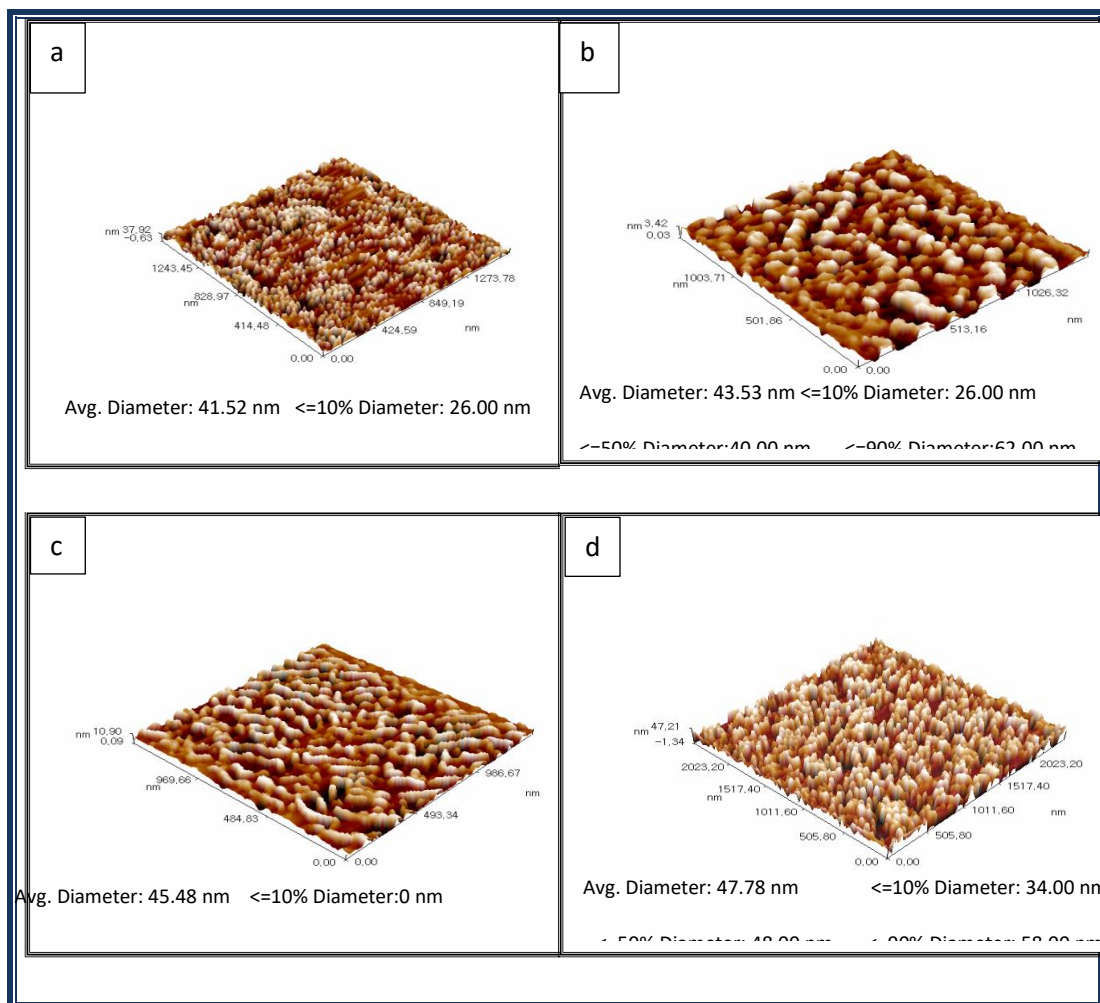


Fig. (7) (3D and particles distribution) AFM of $\text{TiO}_2\text{-Al}_2\text{O}_3$ nanoparticles (a) at 400° C (b) at 500° C (c) at 600° C (d) 700° C

3.1.4 Fourier Transforms Infrared Spectroscopy (FT-IR)

FT-IR spectrum in the range between $(4000\text{-}400)\text{ cm}^{-1}$ was used to characterize the prepared samples, the results showed the existence of hydroxyl groups in samples. The broad peaks centered 3361 cm^{-1} and 3429 cm^{-1} at calcination temperatures (400, and 500)° C respectively are referred to the stretching vibrations of the O–H group, which is attributed to the significant amount of H_2O molecules in the interlayer space and surface [44, 45], and also due to the reaction between the O-H groups of TiO_2 [46]. Another peak of around $(1620\text{ -}1650)\text{ cm}^{-1}$ is attributed to the H-O-H bending mode at the same temperatures above [47]. The Ti–OH vibration band becomes much weaker when calcination temperature has been increased [48]. So TiO_2 calcined at (600, and 700) °C

did not show any aforesaid two broad peaks and it almost completely disappeared at this calcination temperature. That led to the reduced surface area and adsorbed water molecule at high calcination temperature [46].

Two bands at 2854 cm^{-1} , and 2916 cm^{-1} , and band at around 1514 cm^{-1} , are assigned to the asymmetric stretching, and symmetric stretching and bending C–H vibrations respectively at 400°C , can be attributed to the organic residues, also this band appear at 500°C in range 2869 cm^{-1} , 2927 cm^{-1} and 1515 cm^{-1} which remain in TiO_2 even after low calcination temperatures [48],[49]. It is observed that with increasing calcination temperature ($600\text{--}700$) $^\circ\text{C}$ the bands of links stretch will decrease the organic part is degraded with increasing temperature [34]. The broadband from about 400 cm^{-1} , till 1000 cm^{-1} was assigned to Ti–O [44],[34] the peaks appear at range about 1000 cm^{-1} to 1200 cm^{-1} , was assigned Ti–O–Ti skeletal frequency region [50]-[52].

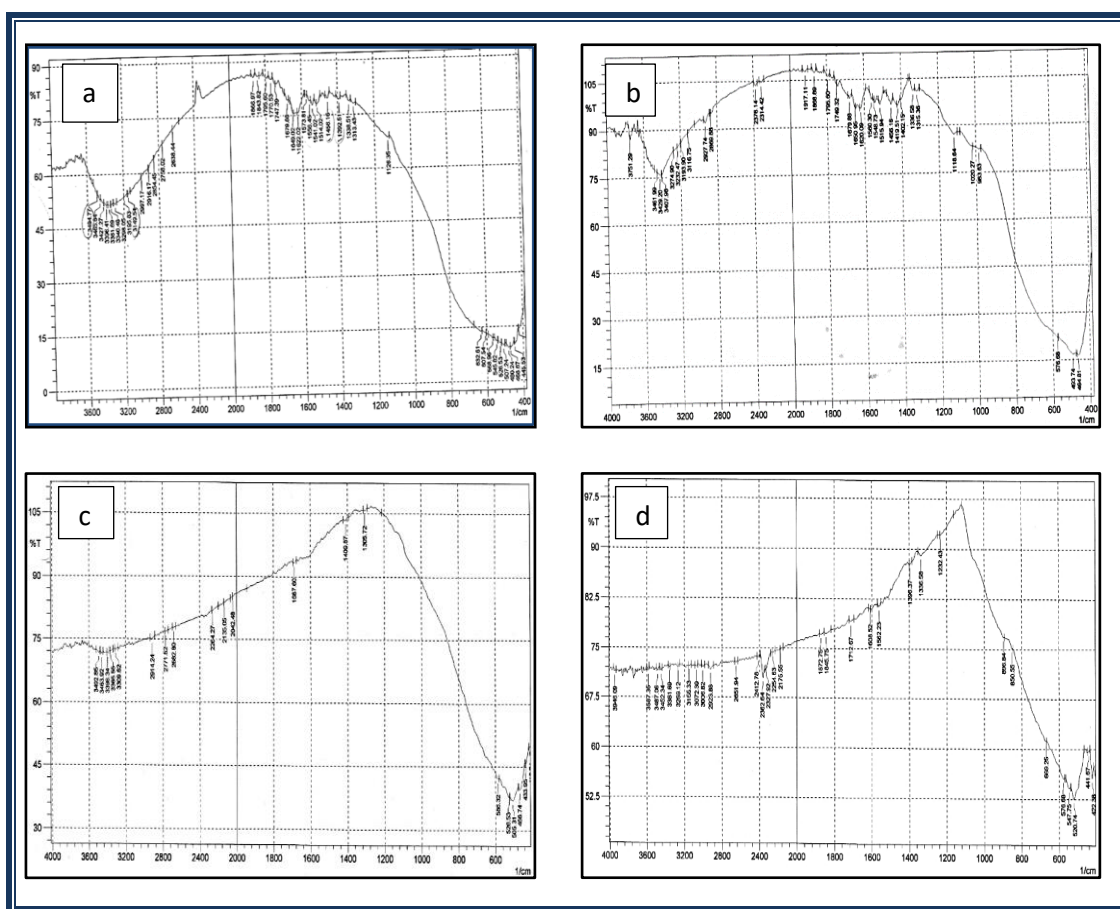


Fig. (8) FTIR spectrum for TiO_2 (a) at 400°C (b) at 500°C (c) at 600°C (d) 700°C

The results of the FTIR spectrum for the $\text{TiO}_2\text{-Al}_2\text{O}_3$ nano composited at calcination temperatures (400, 500, 600, and 700) $^\circ\text{C}$ are shown in Figure (9, a to d) respectively. The pronounced band around (3400, 3427, 3460, and 3490) cm^{-1} at calcination temperatures (400, 500, 600, and 700) $^\circ\text{C}$ respectively, are attributed to the stretching modes for the surface adsorbed water and hydroxyl groups [53],[54], also beak has appeared (1620-1649) cm^{-1} were assigned to bending modes of O–H from the mixed oxides and surface adsorbed water [55]. The –OH absorption peaks become weaker with increasing calcination temperature.

In addition, absorption bands have appeared at a range (1666-1683) cm^{-1} and (1415-1494) indicated the formation of γ -alumina, the intensity of these bands decreased gradually as increasing calcination temperatures, which was attributed to the rapid growth of the crystalline nanoparticles [37].

The low-frequency absorption band at range (424.3- 476.3) cm^{-1} is attributed to the Ti–O vibration of the samples [28]. A broad absorption peak at 500-700 cm^{-1} in all samples which can be assigned to hetero metal-oxygen bonds of –Ti–O–Al– at different temperatures [37] attributed to $\text{TiO}_2\text{-Al}_2\text{O}_3$ the absorption peak still broad with increasing calcination temperature of $\text{TiO}_2\text{-Al}_2\text{O}_3$, the reason for the results that means no broken in Al-Ti-Al bonds [56]. Some weak peak appears around (2717-2935.4) cm^{-1} stretching C–H vibrations, which can be attributed to the organic residues, that remain in the sample after low calcination temperature [57], organic part is degraded with increasing temperature, so these peaks become weaker [34].

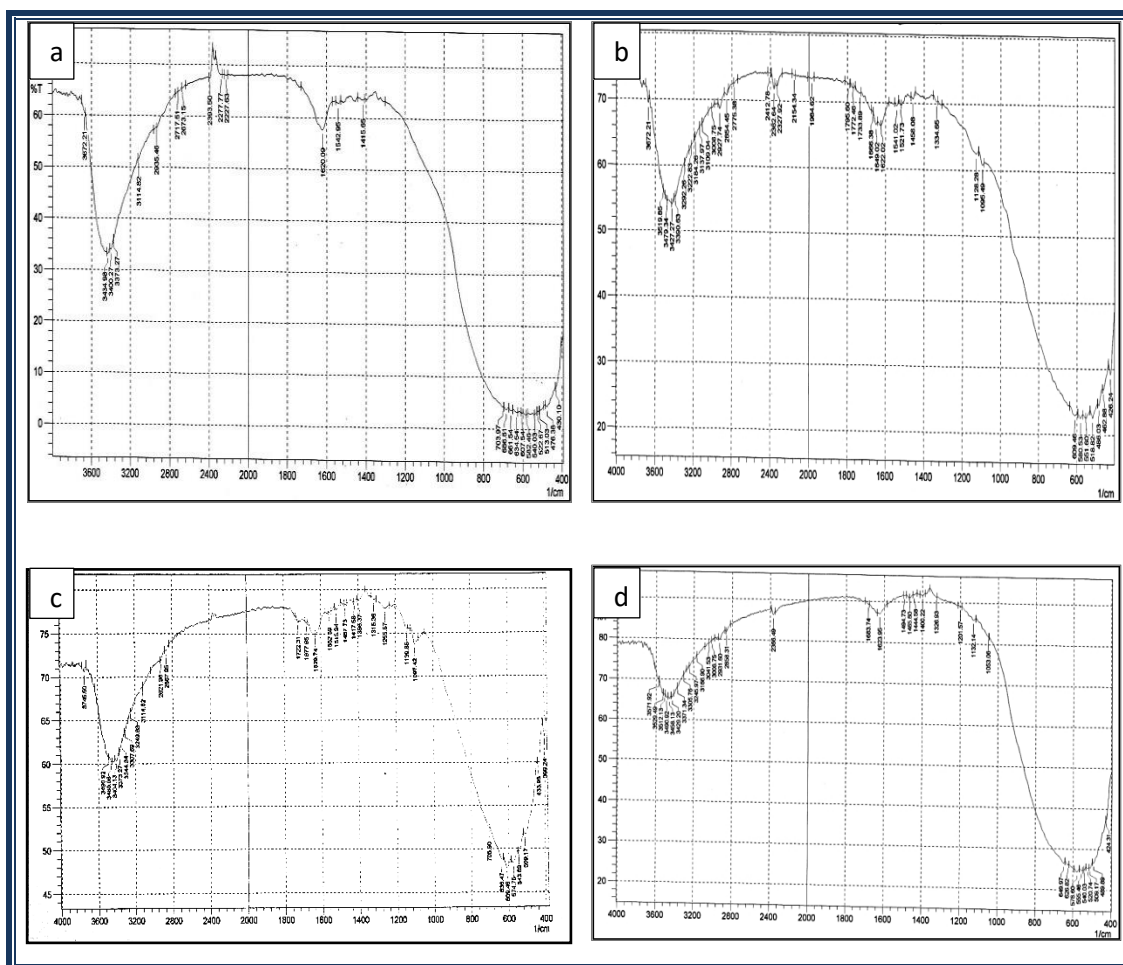


Fig. (9) FTIR spectrum for $\text{TiO}_2\text{-Al}_2\text{O}_3$ (a) at 400° C, (b) at 500° C, (c) at 600° C, (d) 700° C.

4. Effect of Al_2O_3 addition, and calcination temperature

The values of BET surface area, crystal size, particles size, and phase transformation of the prepared samples TiO_2 , and Al_2O_3 are listed in Tables (1), and (2). The prepared pure TiO_2 nanoparticles reported a relatively reduced value of the surface area as compared with the ones of synthesized $\text{TiO}_2\text{-Al}_2\text{O}_3$ nanoparticles. The BET specific surface area of TiO_2 nanomaterials increases with the addition of alumina Figure (10), so the $\text{TiO}_2\text{-Al}_2\text{O}_3$ has a larger surface area under all temperatures (400,500,600,700) °C Table 3.4. This means that the alumina leads to an increase in the surface area of the composites, and that may be due to the distribution of amorphous Al_2O_3 into the TiO_2 lattice crystals; this causes an increase in lattice void among TiO_2 crystals [28]. The highest surface area of $\text{TiO}_2\text{-Al}_2\text{O}_3$ where at calcination temperature 500°C. Table (2) shows that the addition of

Al_2O_3 to TiO_2 surface had a major impact on the specific surface area, as it is noticeably increased from $96.87 \text{ m}^2/\text{g}$ for TiO_2 to $355.18 \text{ m}^2/\text{gm}$. for mixed oxides $\text{TiO}_2\text{-Al}_2\text{O}_3$ at 500°C . Although the crystal size of the $\text{TiO}_2\text{-Al}_2\text{O}_3$ mixed oxide at the temperature of 500°C was bigger than it at the temperature 400°C , the surface area was larger, and this means that the crystal size, is not the main reason that causes the increase in the surface area [28], as the temperature can have an effect on the distribution of alumina within the titanium and it can be observed that from the surface difference between the two temperatures from the SEM. On the other hand, the specific surface area of $\text{TiO}_2\text{-Al}_2\text{O}_3$ decreases with increasing the temperature [39] On the other hand, increasing calcination temperature led to an obvious decrease in the specific surface area of $\text{TiO}_2\text{-Al}_2\text{O}_3$ [41]. The addition of Al_2O_3 also affects the phase transformation of TiO_2 , Pure TiO_2 is anatase at $(400,500)^\circ\text{C}$, and transforms to rutile at 600°C , which was in $\text{TiO}_2\text{-Al}_2\text{O}_3$ mixed oxide the only anatase appeared at all calcined temperatures, this means no phase transformation had occurred [37].

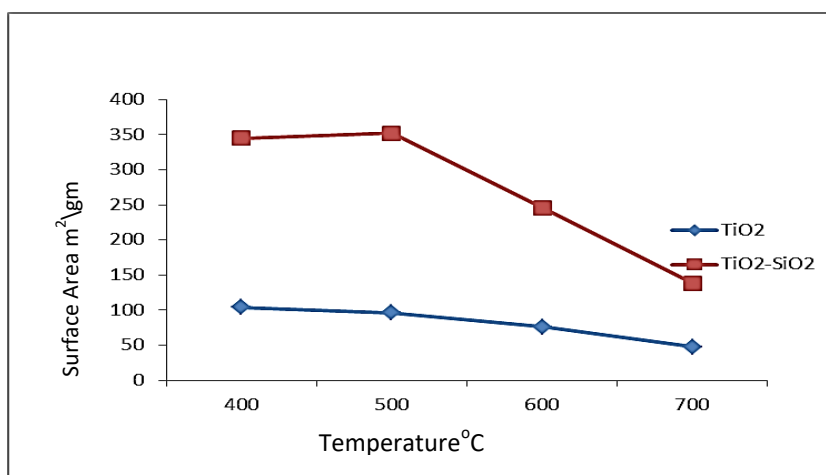


Fig. (10) The effect of adding alumina, and temperatures calcination on the surface area of pure TiO_2

5. Conclusions:

The sol-gel technique was successfully used to prepare TiO_2 and mixed oxides of TiO_2 - Al_2O_3 . The XRD analysis proved a single-phase and crystalline anatase formation for TiO_2 samples calcined at (400°C and 500°C) respectively, and the crystal size of pure titanium increased as temperature increased from 9.20 nm to 37.22nm. The distribution of average particle size, shape of the surface and the presence of nanoparticles in TiO_2 and Al_2O_3 were proved by AFM, while the surface morphologies of TiO_2 and mixed oxides composite were studied by SEM micrographs at a different range of calcination temperatures to agree with AFM results, after alumina addition, particle size was decreased at all temperatures at the same time with increasing temperature from 29 nm at 400 ° C to 46.69 nm at 700°C.

The surface area of both TiO_2 and TiO_2 - Al_2O_3 particles was performed by BET method and showed good results, the addition of Al_2O_3 to TiO_2 led to a significant increase of surface area at a different range of calcination temperatures (400-700) °C, it could be concluded that the higher calcination temperature the lower values of surface area and the relatively larger size of nanoparticles.

The prepared mixed oxides: titanium dioxide cemented with gamma-alumina having a relatively high surface area could be a favorable candidate as catalyst support with high stability for different petroleum refining processes.

References

- [1] Deotale Anjali Jain “Synthesis and Characterization of Some Metal Oxide Nanoparticles” Ph.D thesis, School of Physics Devi Ahilya Vishwavidhyalaya, Indore, India; (2014), (Retrieved in 15 Jul.2017).
- [2] Chikae, M., Idegami, K., Kerman, K., Nagatani, N., Ishikawa M., Takamura, Y., Tamiya, E., "Direct fabrication of catalytic metal nanoparticles onto the surface of a screen-printed carbon electrode" *Electrochemistry Communications*, 8, (2006). 1375-1380
- [3] Rodriguez, J.A., Liu, G., Jirsak, T., Hrbek, J., Chang, Z., Dvorak, J. and Maiti, A., Activation of gold on titania: Adsorption and reaction of SO₂ on Au/TiO₂ (110). *Journal of the American Chemical Society*, 124(18), pp.5242-5250, 2002.
- [4] Mao H, Qiu Z, Shen Z, Huang W. Hydrophobic associated polymer based silica nanoparticles composite with core-shell structure as a filtrate reducer for drilling fluid at ultra-high temperature. *J Pet Sci Eng* 2015; 129:1–14.
- [5] Hendraningrat L, Torseater O. Metal oxide-based nanoparticles: revealing their potential to enhance oil recovery in different wettability systems. *Appl Nanosci* 2015; 5:181–99.
- [6] Khalil M, Lee RL, Liu N. Hematite nanoparticles in aquathermolysis: a desulphurization study of thiophene. *Fuel* 2015; 145:214–20.
- [7] Munawar Khalil, Badrul Mohamed Jan, Chong Wen Tong, Mohammed Ali Berawi, “Advanced nanomaterials in oil and gas industry: Design, application and challenges”. *Applied Energy* 191; 287–310, 2017.
- [8] H. Topsøe, B.S. Clausen, F.E. Massoth, in: J.R. Anderson, M. Boudart (Eds.), “Catalysis Science and Technology”, vol.11, 1996.
- [9] Ghazi M. Abed, Abdulkareem M. A. Alsammarraie, Basim I. Al-Abdaly, “Cr-Gd co-doped TiO₂ Nanoribbons as Photoanode in Making Dye Sensitized Solar Cell”. *Nanoscience and Nanometrology*, 3(1): 27-33, 2017.
- [10] Isao MOCHEDA and Ki-Hyouk CHO, “An Over View of Hydrodesulphurization and Hydrodenitrogenation”. *Journal of Japan petroleum institute* .47. (3).145-163, 2003.
- [11] Maricq, M. M., Chase, R. E., Xu, N. and Laing, P. M., “The effects of the catalytic converter and fuel sulfur level on motor vehicle particulate matter emissions: Light duty diesel vehicles”. *Environmental Science & Technology*, 36: 283 – 289, 2002.
- [12] Zhu, W., Zhu, G., Li, H., Chao, Y., Chang, Y., Chen, G., and Han, C., "Oxidative desulfurization of fuel catalyzed by metal- 818based type ionic liquids", *Molecular Catalysis A: Chemical* 347:8-14, 2011.

- [13] Gray J.H. and Handwerk G. E., "Petroleum Refining Technology and Economics", 2nd Edition ed., Marcel Dekker, Inc, 1984.
- [14] Samya El-Sherbiny, Fatma Morsy, Marwa Samir, Osama A. Fouad. "Synthesis, characterization and application of TiO₂ nanopowders as special paper coating pigment". Appl Nanosci, 4:305–313, 2014.
- [15] Athapon Simpraditpan, Thanakorn Wirunmongkol, Wisuthchai Boonwatcharapunsakun, Sommai Pivsa-art, Churairat Duangduenb, Singto Sakulkaemarue Thai and Sorapong Pavasupree, (2011), Preparation of High Photocatalyst Mesoporous TiO₂ from Nanosheets Using Autoclave Unit (Thai Made), Energy Procedia 9 , 440 – 445.
- [16] Ahmedzeki N S, Hussein SJ, Abdulnabi WA. "Recycling Waste Cans to Nano Gamma Alumina: Effect of the Calcination Temperature and pH" International Journal of Current Engineering and Technology. 2017 Jan .7.1.
- [17] E.Y. Kaneko, S.H. Pulcinelli , V. Teixeira da Silva , C.V. Santilli, "Sol–gel synthesis of titania–alumina catalyst supports". Applied Catalysis A: General 235, 71–78, 2002.
- [18] G. Liang, L. He, H. Cheng et al., "The hydrogenation/dehydrogenation activity of supported Ni catalysts and their effect on hexitols selectivity in hydrolytic hydrogenation of cellulose," Journal of Catalysis, vol. 309, pp. 468–476, 2014.
- [19] Q. Luo, M. Beller, and H. Jiao, "Formic acid dehydrogenation on surfaces—a review of computational aspect," Journal of Theoretical and Computational Chemistry, vol. 12, no. 7, Article ID 1330001, 2013.
- [20] R. Palcheva, L. Dimitrov, G. Tyuliev, A. Spojakina, and K. Jiratova, "TiO₂ nanotubes supported NiW hydrodesulphurization catalysts: characterization and activity," Applied Surface Science, vol. 265, pp. 309–316, 2013.
- [21] Samira Bagheri, Nurhidayatullaili Muhd Julkapli, and Sharifah Bee Abd Hamid, "Titanium Dioxide as a Catalyst Support in Heterogeneous Catalysis", the Scientific World Journal, 2014.
- [22] G. Murali Dhar, B.N. Srinivas, M.S. Rana, Manoj Kumar, S.K. Maity, "Mixed oxide supported hydrodesulfurization catalysts—a review", Catalysis Today 86, 45–60, 2003.
- [23] Koo, J. H. "Fundamentals, Properties, and Applications of Polymer Nanocomposites" Cambridge University Press, (2016), pg. 12. (Chapter.1, Retrieved in 13 May 2018).
- [24] Wang, Y., Wang, R., Guo, C., Miao, J., Tian, Y., Ren, T. and Liu, Q., "Pathdirected and maskless fabrication of ordered TiO₂ nanoribbons", Nanoscale, 4(5), pp.1545-1548, 2012.
- [25] Athapon Simpraditpan, Thanakorn Wirunmongkol, Wisuthchai Boonwatcharapunsakun, Sommai Pivsa-art, Churairat Duangduenb, Singto Sakulkaemarue Thai and Sorapong Pavasupree, "Preparation of High Photocatalyst Mesoporous TiO₂ from Nanosheets Using

- Autoclave Unit (Thai Made)", Energy Procedia 9 , 440 – 445, 2011.
- [26] Mehdi Karimi, Fakhry Seyedeyn-Azad and Jalal Abedi., "Removal of mercaptans from gas–oil using synthesised anatase form of TiO₂ nanoparticles. the canadian journal of chemical engineering. Vol. 91, 2013.
- [27] Nadzirah, S., Foo, K.L. and Hashim, U., "Morphological reaction on the different stabilizers of titanium dioxide nanoparticles", Int J Electrochem Sci, 10, pp.5498-5512, 2015.
- [28] Wenjie Zhang, Chuanguo Li and Ruyuan Li. (2015). Sol-gel Preparation of TiO₂-Al₂O₃ Composite Materials to Promote Photocatalytic Activity. Nanoscience & Nanotechnology-Asia, 5, 8-14, 2015.
- [29] Marina Teixeira Laranjo, Natalia Carminati Ricardi, Leliz Ticono Arenas, Edilson Valmir Benvenuti , Matheus Costa de Oliveira , Marcos Jose´ Leite Santos , Tania Maria Haas Costa. "TiO₂ and TiO₂/SiO₂ nanoparticles obtained by sol–gel method and applied on dye sensitized solar cells", J Sol-Gel Sci Technol 72:273–281, 2014.
- [30] Petushkov, A., "Synthesis and Characterization of Nanocrystalline and Mesoporous Zeolites", s.l.:Doctoral PhD. Dissertation, University of Iowa, 2011.
- [31] Ba-Abbad, M.M., et al.: Synthesis and catalytic activity of TiO₂ nanoparticles for photochemical oxidation of concentrated chlorophenols under direct solar radiation. Int J Electrochem 7, 4871–4888, 2012.
- [32] Yung-Fang Chena, Chi-Young Lee, Ming-Yu Yeng, Hsin-Tien Chiu, "The effect of calcination temperature on the crystallinity of TiO₂ nanopowders. Journal of Crystal Growth 247 363–370, 2003.
- [33] Samya El-Sherbiny, Fatma Morsy, Marwa Samir, Osama A. Fouad. "Synthesis, characterization and application of TiO₂ nanopowders as special paper coating pigment". Appl Nanosci, 4:305–313, 2014.
- [34] João Victor Marques Zoccal, Fábio de Oliveira Arouca, José Antonio Silveira Gonçalves. "Synthesis and characterization of TiO₂ nanoparticles by the method pechini". Materials Science Forum Vols 660-661: pp 385-390, 2010.
- [35] Ali Mahyar, Mohammad Ali Behnajade and Naser Modirshahla. "Characterization and photocatalytic activity of SiO₂-TiO₂ mixed oxide nanoparticles prepared by sol-gel method", Indian Journal of chemistry, Vol. 49A, PP 1593-1600, 2010.
- [36] B.N.Srinivas, S.K.Maity, V.V.D.N.Prasad, M.S.Rana, Manoj Kumar, G.Murali Dhar and T.S.R.Prasada Rao, "Support effect studies on TiO₂-Al₂O₃ mixed oxide hydroprocessing catalysts", Studies in Surface Science and Catalysis, Vol. 113, 1998.
- [37] Chengwu Yang , Qian Zhang , Jun Li , Ruirui Gao , Zhe Li, Wei Huang, "Catalytic activity

- and crystal structure modification of Pd/ γ -Al₂O₃–TiO₂ catalysts with different Al₂O₃ contents”, *Journal of Energy Chemistry*. 25, 375–380, 2016.
- [38] Kaile Wang, Bolun Yang, Yu Liu, and Chunhai Yi, “Preparation of Ni₂P/TiO₂-Al₂O₃ and the Catalytic Performance for Hydrodesulfurization of 3-Methylthiophene”, *Energy Fuels*, 23, 4209–4214, 2009.
- [39] J.S. Tobin, A.J. Turinske, N. Stojilovic, A.F. Lotus b, G.G. Chase., “Temperature-induced changes in morphology and structure of TiO₂-Al₂O₃ fibers”. *Current Applied Physics* 12, 919-923, 2012.
- [40] Wenjie Zhang, Ruyuan Li, Hongbo He, “Synthesis of Mesoporous TiO₂-Al₂O₃ Binary Oxides Photocatalyst by Sol-Gel Method Using PEG1000 as Template”. *International Journal of Photoenergy*, Volume 2012, Article ID 108175, 7 pages, 2012.
- [41] Sahbeni K, Sta I, Jlassi M, Kandyla M, Hajji M, Kompitsas M, and Dimassi W, “Annealing Temperature Effect on the Physical Properties of Titanium Oxide Thin Films Prepared by the Sol-Gel Method”. *Journal of Physical Chemistry & Biophysics*, Volume 7, Issue 3, 2017.
- [42] Dang Mau Chien, Nguyen Ngoc Viet, Nguyen Thi Kieu Van and Nguyen Thi Phuong Phong, “Characteristics modification of TiO₂ thin films by doping with silica and alumina for self-cleaning application”. *Journal of Experimental Nanoscience*, Vol. 4, No. 3, 221–232, 2009.
- [43] Meryem Polat Gonullu, Hakan Ates, “The characteristic evolution of TiO₂/Al₂O₃ bilayer films produced by ALD: Effect of substrate type and wide range annealing temperature”. *Superlattices and Microstructures* 142, 106529, 2020.
- [44] Manasi Manoj Karkare, “Choice of precursor not affecting the size of anatase TiO₂ nanoparticles but affecting morphology under broader view”, *Int Nano Lett.* 4:111, 2014.
- [45] Sauvet, A.L., Baliteau, S., Lopez, C. and Fabry, P., “Synthesis and characterization of sodium titanates Na₂Ti₃O₇ and Na₂Ti₆O₁₃”. *Journal of Solid State Chemistry*, 177(12), pp.4508-4515, 2004.
- [46] Adawiya Haider, Riyadh Al-Anbari, Ghadah Kadhim, Zainab Jameel, “Synthesis and photocatalytic activity for TiO₂ nanoparticles as air purification”. *MATEC Web of Conferences* 162, 05006, 2018.
- [47] Huang, C., Bai, H., Huang, Y., Liu, S., Yen, S., & Tseng, Y., “Synthesis of neutral SiO₂/TiO₂ hydrosol and its application as antireflective self-cleaning thin film”. *International Journal of Photoenergy*, 2012. <http://doi.org/10.1155/2012/620764>.
- [48] Yung-Fang Chena, Chi-Young Lee, Ming-Yu Yeng, Hsin-Tien Chiu, “The effect of calcination temperature on the crystallinity of TiO₂ nanopowders”. *Journal of Crystal Growth* 247, 363–370, 2003.

- [49] Yodyingyong, S., et al., “Physicochemical Properties of Nanoparticles Titania from Alcohol Burner Calcination”. *Bull. Chem. Soc. Ethiop* 25(2), 263–272 (ISSN 1011-3924), 2011.
- [50] Ali Amoozadeh ,Elham Tabrizian, Saeedeh Shahjoe, “Nickel(II) Schiff base complex supported on nano-titanium dioxide: A novel straightforward route for preparation of supported Schiff base complexes applying 2,4- toluenediisocyanate”. *Appl Organometal Chem.* p(1 of 9), 2019.
- [51] Azadeh Ebrahimian Pirbazaria,b, Pejman Monazzama., Behnam Fakhari Kisomi, “Co/TiO₂ nanoparticles: preparation, characterization and its application for photocatalytic degradation of methylene blue”. *Desalination and Water Treatment*, 63, 283–292, February, 2016.
- [52] Bingbing Guan Jie Yu Siyao Guo, Shen Yua and Song Han, “Porous nickel doped titanium dioxide nanoparticles with improved visible light photocatalytic activity”. *The Royal Society of Chemistry, Nanoscale Adv*, 2, 1352–1357, 2020.
- [53] Venkatachalam, N.; Palanichamy, M.; Arabindoo, B., “Alkaline earth metal doped nanoporous TiO₂ for enhanced photocatalytic mineralization of bisphenol-A. *Catal*” .Comm. 8, 1088-1093, 2007.
- [54] Venkatachalam, N.; Palanichamy, M.; Murugesan, V., “Sol-gel preparation and characterization of alkaline earth metal doped nano TiO₂: Efficient photocatalytic degradation of 4- chlorophenol”. *J. Mol. Catal. A.*, 273, 177-185, 2007.
- [55] Ahmed, M. A., & Abdel-Messih, M. F., “Structural and nano-composite features of TiO₂–Al₂O₃ powders prepared by sol–gel method”. *Journal of Alloys and Compounds*, 509(5), 2154-2159, 2011.
- [56] Huang Y X. and Senos M R *mater Res Bull*, 37. (2000), 99.
- [57] D.V Sridevi, V Ramesh, T Sakthivel, K Geetha, V Ratchagar, K Jagannathan, K Rajarajan, K Ramachadran, “Synthesis, Structural and Optical Properties of Co Doped TiO₂ Nanocrystals by Sol-Gel Method. *Mechanics*”, *Materials Science & Engineering Journal, Magnolithe*, 9 (1), 10.2412/mmse.99.9.726. Hal-01496431, 2017.